Energy dissipating flows for solving nonlinear eigenpair problems

Ido Cohen *, Guy Gilboa

Technion – Israel Institute of Technology, Haifa 32000, Israel

ARTICLE INFO

ABSTRACT

This work is concerned with computing nonlinear eigenpairs, which model solitary waves and various other physical phenomena. We aim at solving nonlinear eigenvalue problems of the general form $T(u) = \lambda Q(u)$. In our setting T is a variational derivative of a convex functional (such as the Laplacian operator with respect to the Dirichlet energy), Q is an arbitrary bounded nonlinear operator and λ is an unknown (real) eigenvalue. We introduce a flow that numerically generates an eigenpair solution by its steady state.

Analysis for the general case is performed, showing a monotone decrease in the convex functional throughout the flow. When T is the Laplacian operator, a complete discretized version is presented and anlalyzed. We implement our algorithm on *Korteweg and de Vries* (KdV) and *nonlinear Schrödinger* (NLS) equations in one and two dimensions. The proposed approach is very general and can be applied to a large variety of models. Moreover, it is highly robust to noise and to perturbations in the initial conditions, compared to classical Petiashvili-based methods.

© 2018 Elsevier Inc. All rights reserved.

1. Introduction

Nonlinear elliptic equations arise in various problems in physics, e.g. for stationary solutions of equations, such as *Bose–Einstein condensates* (BEC), *nonlinear Schrödinger* (NLS) and *Korteweg and de Vries* (KdV) [1]. In this work we focus on nonlinear problems of the form,

$$T(u) = \lambda Q(u), \tag{1}$$

where u is a function in a Banach space $\mathcal{U}$, and T and Q are (possibly) nonlinear operators. More specifically, we assume T to be a subgradient of a convex, proper, lower-semi-continuous functional J,

$$T(u) \in \partial_u J(u), \tag{2}$$

where $\partial_u J(u)$ denotes the subdifferential of $J(u)$. On the right-hand-side of (1), $Q : \mathcal{U} \to \mathcal{U}$ is a bounded (possibly) nonlinear operator. We refer to functions u which admit (1) as eigenfunctions, with a corresponding eigenvalue $\lambda \in \mathbb{R}$. Our aim is to find a pair $(u, \lambda) \in \mathcal{U} \times \mathbb{R}$ that admits (1), referred to as an *eigenpair*.

---

* Corresponding author.
E-mail addresses: ido.coh@gmail.com (I. Cohen), guy.gilboa@ee.technion.ac.il (G. Gilboa).

Eigenpairs of nonlinear operators appear in various fields of science and engineering. Their analysis can provide deeper understanding and significant insights related to nonlinear systems. Nonlinear eigenvalue analysis is an active field of research, from both a theoretical and a computational perspective. In some nonlinear problems, such as [2] the underlying operators are linear but the dependency on λ is nonlinear. A recent review of such *nonlinear eigenvalue problems* (NEP) appear in [3]. These studies are part of a different branch of problems (not in the scope of this paper). We examine solutions which can be formulated by Eq. (1), where the eigenvalue is linearly dependent. We summarize below the main related studies.

1.1. Solitary waves as solutions of nonlinear eigenvalue problems

A pioneering work in this field, which was followed by many, is that of Petviashvili [4]. It was aimed at finding numerical approximations of stationary solutions for the Kadomtsev–Petviashvili equation with positive dispersion (KPI equation). The method, originally, was develop to obtain stationary solutions of wave equations of the form

$$-Mu + u^p = 0, \tag{3}$$

where M is a positive, self-adjoint operator and p is a constant. We note that M should be invertible, as the iterative procedure is based on its inversion. Conditions for the convergence of Petviashvili's method were established in [5]. The approach of Petviashvili was later generalized and applied to a family of nonlinear problems, such as [6–9]. However, all these algorithms assume M is invertible. Moreover, it is not aimed at finding eigenpairs, but at solving a more restricted problem. When casted within the formulation of (1), the eigenvalue is set to a unit value ($\lambda = 1$). Our proposed method is based on a forward flow, and hence M is not require to be invertible. Moreover, it is aimed at finding eigenpairs, of unknown λ. The resulting eigenpair is related to an initial condition, provided by the user, which can emerge from noisy experimental data, for instance.

Yang and Lakoba [7,10,11] generalized Petviashvili's iteration method, accelerated the inverse power method and used modified conjugate gradient to find solitary waves. In [12] it was suggested to combine the conjugate gradient method with accelerated inverse power method into a unified algorithm, which coincides with Petviashvili's method for small enough error. This method was shown to provide fast convergence rates. In our work we compare the numerical results to this method and to a modified version of it for adaptively computing eigenpairs. The focus of this paper is on the robustness of the methods, rather than on the convergence rate. We note that our forward flow requires considerably more iterations to converge, compared to algorithms based on inversion. However, it is much more stable and general.

1.2. Variational formulations of eigenpair problems

Eigenvalue problems are often analyzed theoretically and solved numerically based on energy minimization methods. Within a variational setting, it can be shown that an eigenpair is an extremum of a generalized Rayleigh quotient [13]. This extends in a natural manner to the linear case, where any eigenvector v of a Hermitian matrix A, admitting $Av = \lambda v$, is an extremal point of the associated Rayleigh quotient $R(v) = (v^*Av)/(v^*v) = \lambda$, where v^* is the conjugate transpose of v. The studies of [14–17] aim at finding a minimum (or a local minimum) of an energy functional associated to the eigenvalue problem. In [14,15] a constrained steepest descent is used for solving ground states of BEC. Alternative approaches, such as [16,17], are based on constrained energy minimization techniques with a suitable Lagrange function. In the above cases, both sides of the eigenvalue problem (1) should have an associated energy. This puts some limitations on the variety of problems that can be solved. In our work this restriction is relaxed (so only the operator T is associated with an energy term).

1.2.1. Eigenpairs associated with total variation

The *total variation* (TV) functional, $J_{TV} = \int |\nabla u(x)| dx$, has been thoroughly investigated in recent decades [18]. Since its introduction to the image processing field for denoising and deconvolution by [19], it has been used as an edge preserving regularizer for algorithms related to stereo imaging, optical flow, segmentation and many other computer vision tasks [20]. Eigenpairs associated with TV were investigated in [21] and [22]. It was shown that convex disk-like shapes are eigenfunctions of the nonlinear eigenvalue problem

$$T(u) = \lambda u, \quad T(u) \in \partial_u J_{TV}(u),$$

where $\partial_u J_{TV}(u)$ is the subdifferential of TV. For smooth, non-vanishing gradient, we have $\partial_u J_{TV}(u) = -\text{div}(\nabla u/|\nabla u|)$, which is the 1-Laplacian operator. In recent years, a theory of nonlinear transforms for one-homogeneous functionals has been formulated [23–25]. It is based on the analysis of nonlinear eigenvalue problems. The work of [26] proposed a flow for finding eigenfunctions of one-homogeneous functionals, and is described in more detail below. Numerical methods for finding p-Laplacian eigenpairs were proposed in [27] and [28]. Solutions of semilinear elliptic eigen-problems were presented in [1]. Ground states of generalized eigenvalue problems, which may involve also a smoothing kernel, were analyzed in [29]. An iterative algorithm for finding nonlinear eigenpairs by an extended inverse-power method was proposed by [30]. All of these methods are based partially or mostly on the fact that the eigenpair satisfies an extremum of the associated (generalized) Rayleigh quotient.

Our work generalizes the flow of [26]. It goes beyond the variational setting and allows the nonlinear operator Q in Eq. (1) to be very general.

1.3. Main contributions

The main contributions of this work are as follows:

1. A new flow is introduced, which generates eigenpairs admitting (1). A decrease in the convex functional J associated with the operator T is shown in the continuous setting, under mild assumptions (Sec. 2). When J is a regularizing term, such as the Dirichlet energy, we get a dissipating flow which ensures robustness against noise and stability of the algorithm.
2. The need to omit residual parts perpendicular to the operator T are explained. The concept of the Q^* subspace, where all eigenfunctions must reside in, is introduced (Sec. 2.4). A complementary flow which directs the function u to this subspace is presented and combined with the main flow (Sec. 2.5, Sec. 3).
3. A discrete explicit implementation is proposed and analyzed, when T is the negative Laplacian. We formulate a time step bound that guarantees the monotonic decrease of J throughout the flow (Sec. 4).
4. We employ our algorithm on KdV and NLS equation and draw a comparison between our algorithm and *Newton conjugate gradient methods* (NCGM) [12] in one and two dimensions, showing excellent stability of the flow, for various initial conditions (Sec. 5).

2. Flows for generating eigenpairs

2.1. Preliminary notations and definitions

We first introduce some standard definitions and notations used in this paper. Let Ω be a bounded subset of $\mathbb{R}^N$. We use the L^2 inner product, $\langle u, v \rangle = \int_\Omega uv \cdot d\mathbf{x}$ and its associated norm $\|u\| = \sqrt{\langle u, u \rangle}$. Let $J : \mathcal{U} \to \mathbb{R}$ be a convex functional. We denote by $\partial J(u)$ the subdifferential set of J at u. Let us recall the subgradient inequality: For any $p \in \partial J(u)$, the following inequality holds:

$$J(v) \geq J(u) + \langle p, v - u \rangle. \tag{4}$$

The set of all a for which this inequality holds is the subdifferential. A necessary and sufficient condition for u to be a global minimum of J is if zero is contained in $\partial J(u)$. We recall the "chain rule" for the differentiation of functionals (see Lemma 3.3 of Brezis [31] and recent extensions e.g. in [32]). Let J be a convex, lower semi-continuous, proper functional, $\tau > 0$, and $u \in W^{1,2}((0, \tau); \mathcal{U})$. Let also $p \in L^2((0, \tau); \mathcal{U})$, such that $p \in \partial J(u(t)) a.e.$ in $(0, \tau)$. Then the function $J \circ u : [0, \tau] \to \mathbb{R}$ is absolutely continuous in $[0, \tau]$ with:

$$\frac{d}{dt} J(u(t)) = \langle p, u_t \rangle \quad \forall p \in \partial J(u(t)) \quad a.e. \text{ in } (0, \tau). \tag{5}$$

2.2. Nossek & Gilboa flow

Our work generalizes the work of Nossek & Gilboa [26], for which J is assumed to be convex, absolutely one-homogeneous functional and $Q(u) = u$. We briefly describe this flow and its main properties. The flow is given by,

$$u_t = \frac{u}{\|u\|} - \frac{T(u)}{\|T(u)\|}, \quad T(u) \in \partial_u J, \quad u(0) = f, \tag{6}$$

where f admits $\|f\| \neq 0$ and has zero mean. If J is invariant to a global constant change, i.e. $J(u) = J(u + c)$, $\forall c \in \mathbb{R}$, the solution $u(t)$ of this flow has the following properties:

1. The mean value of $u(t)$ is preserved throughout the flow:

$$\langle u(t), 1 \rangle = 0.$$

2. The value of $J(u(t))$ is decreasing with time

$$\frac{d}{dt} J(u(t)) \leq 0, \ a.e. \ in \ (0, \infty)$$

where equality is reached iff u is an eigenfunction.
3. The L^2 norm of the solution is increasing with time,

$$\frac{d}{dt} \|u(t)\|^2 \geq 0,$$

where equality is reached iff u is an eigenfunction.

4. A steady-state, $u_t = 0$, holds iff u is an eigenfunction.

For further details see [26]. Aujol et al. [33] analyzed the flow and proposed a modification for which existence and uniqueness of the continuous flow can be shown as well as convergence of the discrete iterative algorithm. Following this, we now turn to formulate the main flow which is designed to find solutions for Eq. (1). We will see later that an auxiliary (complementary) flow is required for this generalization to work properly, in order to allow minimal assumptions regarding the operator Q.

2.3. The main flow

We introduce a flow which generates eigenpairs of the form of Eq. (1). Given some initial condition $u(t = 0) = f$, $u(t)$ is evolved by the following PDE,

$$u_t(t) = M(u(t)), \tag{7}$$

where

$$M(u) = s\frac{Q(u)}{\|Q(u)\|} - \frac{T(u)}{\|T(u)\|},$$

and $s = \text{sign}(\langle Q(u), T(u)\rangle)$.

Theorem 1. *Assuming the flow of Eq.* (7) *exists and is unique and* $J(u)$ *satisfies Eq.* (5)*, the solution* $u(t)$ *has the following attributes:*

1. *The value of* J *is decreasing with time,*

   $$\frac{d}{dt}J(u) \leq 0, \ a.e. \ in \ (0, \infty),$$

   where equality is reached iff u admits Eq. (1)*.*
2. *A necessary condition for steady state* $u_t = 0$ *holds iff u is an eigenfunction.*

Proof. We denote $T = T(u(t))$, $Q = Q(u(t))$.

1. From (5) and (7) we deduce,

$$\begin{aligned}
\frac{d}{dt}J(u) &= \langle T, u_t \rangle \\
&= \langle T, s\frac{Q}{\|Q\|} - \frac{T}{\|T\|}\rangle \\
&= \frac{|\langle T, Q\rangle|}{\|Q\|} - \|T\| \leq 0, \quad \text{a.e. in } (0, \infty).
\end{aligned} \tag{8}$$

J is decreasing with time since J is lower-semi-continuous and the derivative is negative a.e. If u is an eigenfunction in the sense of Eq. (1), then the eigenvalue λ can be evaluated by using (1) and taking the inner-product with respect to either Q or T, to have,

$$\lambda = \frac{\langle T, Q\rangle}{\|Q\|^2} = \frac{\|T\|^2}{\langle T, Q\rangle} = \text{sign}(\langle T, Q\rangle)\frac{\|T\|}{\|Q\|}. \tag{9}$$

This yields $|\langle T, Q\rangle| = \|Q\| \cdot \|T\|$ and therefore $(d/dt)J(u) = 0$. Conversely, if $(d/dt)J(u) = 0$ then, following (8),

$$|\langle T, Q\rangle| = \|T\| \cdot \|Q\|,$$

i.e., Q and T are collinear and u admits Eq. (1), hence an eigenfunction.
2. If u admits Eq. (1) then we can assign $T = \lambda Q$ with λ evaluated by the expression on the right of Eq. (9) to get $u_t = M(u) = 0$ in (7). Conversely, let $u_t = 0$ then T and Q are collinear, hence we reach Eq. (1). $\square$

2.4. The space of solutions $\mathcal{Q}^*$

Theorem 1 guarantees certain stability of the flow, since $J(u)$ decreases with time. In addition, the flow stops at an eigenpair, which is our aim. We will see in the analysis below that u needs to be in a certain subspace of $\mathcal{U}$, otherwise, one will attain only trivial solutions of zero eigenvalue. We begin by stating some definitions and notations. Let us define two subsets of $\mathcal{U}$, $\mathcal{T}^\perp$ and $\mathcal{Q}^*$, associated with the operators T and Q.

Definition 1. Let $\mathcal{T}^{\perp}$ be the set perpendicular to the image of the operator T:

$$\mathcal{T}^{\perp} = \{v \in \mathcal{U} : \langle T(u), v \rangle = 0, \forall u \in \mathcal{U}\}.$$

We note that $\mathcal{T}^{\perp}$ is a linear subspace. This can be shown by taking two functions in that set $v_1, v_2 \in \mathcal{T}^{\perp}$ and observing that the following relation holds:

$$\langle T(u), \alpha_1 v_1 + \alpha_2 v_2 \rangle = \alpha_1 \langle T(u), v_1 \rangle + \alpha_2 \langle T(u), v_2 \rangle = 0, \quad \forall u \in \mathcal{U}, \alpha_1, \alpha_2 \in \mathbb{R}.$$

We can now denote a basis for $\mathcal{T}^{\perp}$.

Definition 2. Let $\mathcal{B}$ be an orthonormal basis of $\mathcal{T}^{\perp}$.

Lemma 1. *Let $\mathcal{T}^{\perp}$ be defined as in Definition 1, then:*

1. $J(u)$ *is invariant to addition of $v \in \mathcal{T}^{\perp}$, i.e.:*

$$J(u) = J(u + v), \qquad \forall u \in \mathcal{U}, \forall v \in \mathcal{T}^{\perp}.$$

2. *If the following two conditions hold: (i) The operator T is self-adjoint. (ii) For any minimizer u of J, the subdifferential set, $\partial_u J(u)$, has a single element. Then $\mathcal{T}^{\perp} = \arg\min\{J(u)\}$.*

Proof.   1. As $J(u)$ is convex then, based on the subdifferential inequality (4), we have

$$J(u) \geq J(u + v) - \langle T(u + v), v \rangle = J(u + v), \qquad \forall v \in \mathcal{T}^{\perp},$$

and

$$J(u + v) \geq J(u) + \langle T(u), v \rangle = J(u), \qquad \forall v \in \mathcal{T}^{\perp}.$$

2. If $u \in \arg\min\{J\}$ and $v \in \mathcal{T}^{\perp}$ then:

$$\begin{aligned}
J(u) &\geq J(v) + \langle T(v), (u - v) \rangle \\
&= J(v) + \langle T(v), u \rangle \\
&= J(v) + \langle v, T(u) \rangle \\
&= J(v),
\end{aligned}$$

but as u minimizes J we also have $J(v) \geq J(u)$, therefore $J(v) = J(u)$ and $v \in \arg\min\{J\}$. Conversely, if $u \in \arg\min\{J\}$ then $T(u) = 0$, since T is self-adjoint we get

$$\langle T(u), v \rangle = \langle u, T(v) \rangle = 0, \quad \forall v \in \mathcal{U}. \quad \square$$

Corollary 1. *Let the conditions of Lemma 1, item 2 hold and $\min\{J(u)\} = 0$, then:*

1. $\mathcal{T}^{\perp}$ *is the null space of $J(u)$.*
2. $J(u)$ *is invariant to addition of elements in the null space.*

We would now like to define a second significant subset, denoted by $\mathcal{Q}^*$.

Definition 3. Let $\mathcal{Q}^*$ be defined by

$$\mathcal{Q}^* = \{u \in \mathcal{U} : \langle Q(u), e_i \rangle = 0 \quad \forall e_i \in \mathcal{B}\},$$

where $\mathcal{B}$ is defined in Definition 2 and e_i are its orthonormal elements.

We would now like to define an energy which measures how far we are from $\mathcal{Q}^*$:

$$E(u) = \frac{1}{2} \sum_{e_i \in \mathcal{B}} \langle Q(u), e_i \rangle^2. \tag{10}$$

Remark 1. An alternative definition of $\mathcal{Q}^*$ is the null space of the energy functional $E(u)$.

We observe that every $v \in \mathcal{T}^{\perp}$ is perpendicular to $Q(u^*)$ where u^* is an eigenfunction with $\lambda \neq 0$. This is a straightforward consequence of Eq. (1) and Definition 1. Hence, $\lambda \langle Q(u^*), e_i \rangle = \langle T(u^*), e_i \rangle = 0$. We can summarize this by the following statement:

Remark 2. All eigenfunctions with nonzero eigenvalue belong to $\mathcal{Q}^*$.

Example. Let us demonstrate the sets $\mathcal{T}^{\perp}$ and $\mathcal{Q}^*$ by examining the classical case where $T = -\Delta$ (the negative Laplacian operator) with Neumann boundary conditions. We have $\langle \Delta u, v \rangle = 0$ for all functions v which are identically constant. Thus we get

$$\mathcal{T}^{\perp} = \{v \in \mathcal{U}: \quad v = const\},$$

and the basis of $\mathcal{T}^{\perp}$ is $\{1\}$. Consequently,

$$\mathcal{Q}^* = \{u \in \mathcal{U}: \langle Q(u), 1 \rangle = 0\}.$$

Proposition 1. *Let $\mathcal{Q}^*$ be defined as in Definition 3 and $u(t)$ evolves according to Eq. (7). If $u(t)$ is not an eigenfunction with $\lambda = 0$, then the following properties hold for all $t \in (0, \infty)$:*

1. *If $u(t) \notin \mathcal{Q}^*$ then $(d/dt) J(u(t)) < 0$.*
2. *If $u(t) \in \mathcal{Q}^*$ then the projection of $u(t)$ on the linear space $\mathcal{T}^{\perp}$ is preserved throughout the flow (Eq. (7)). In other words:*

$$\langle u(t), v \rangle = const, \quad \forall v \in \mathcal{T}^{\perp}.$$

Proof. 1. If $u \notin \mathcal{Q}^*$ then $\exists e \in \mathcal{B}$ s.t. $\langle Q(u), e \rangle \neq 0$. Let us denote the projection of $Q(u)$ on $\mathcal{T}^{\perp}$ as,

$$Q^{\perp}(u) = \sum_{e_i \in \mathcal{B}} e_i \cdot \langle Q(u), e_i \rangle \neq 0,$$

and the complement (parallel) part as,

$$Q^{\parallel}(u) = Q(u) - Q^{\perp}(u).$$

The time derivative of $J(u)$ is therefore,

$$
\begin{aligned}
\frac{d}{dt} J(u) &= \langle T(u), u_t \rangle \\
&= \langle T(u), s \frac{Q(u)}{\|Q(u)\|} - \frac{T(u)}{\|T(u)\|} \rangle \\
&= \frac{|\langle T(u), Q(u) \rangle|}{\|Q(u)\|} - \|T(u)\| \\
&= \frac{|\langle T(u), Q^{\parallel}(u) \rangle|}{\sqrt{\|Q^{\parallel}(u)\|^2 + \|Q^{\perp}(u)\|^2}} - \|T(u)\| < 0.
\end{aligned}
$$

As long as $T(u) \neq 0$ the time derivative of $J(u)$ is negative since $Q^{\perp}(u) \neq 0$. The time derivative is zero only when $T(u) = 0$ (where $J(u)$ reaches its global minimum) and therefore $\lambda = 0$.

2. Let us compute the derivative of $\langle u(t), v \rangle$ with respect to time:

$$\frac{d}{dt} \langle u(t), v \rangle = \langle u_t, v \rangle = \langle s \frac{Q(u)}{\|Q(u)\|} - \frac{T(u)}{\|T(u)\|}, v \rangle = s \frac{\langle Q(u), v \rangle}{\|Q(u)\|} - \frac{\langle T(u), v \rangle}{\|T(u)\|}.$$

If $v \in \mathcal{T}^{\perp}$ then $\langle T(u), v \rangle = 0$ and since $u \in \mathcal{Q}^*$ then $\langle Q(u), v \rangle = 0$. Consequently,

$$\frac{d}{dt} \langle u(t), v \rangle = 0 \quad \Rightarrow \quad \langle u(t), v \rangle = const. \quad \square$$

Corollary 2. *Let T be a self adjoint operator and $\min\{J(u)\} = 0$. If $u(t)$, the solution of the main flow Eq. (7), admits $u(t) \in \mathcal{Q}^*$, then its projection on the null space of J is preserved.*

This corollary is a generalization of the first attribute of the Nossek & Gilboa flow which guarantees that the mean of u is preserved. A more significant consequence of Proposition 1 is that *if $u \notin \mathcal{Q}^*$ the main flow can reach a steady state only at "trivial" eigenfunctions, with $\lambda = 0$.* This leads us to propose a complementary flow which retains $u \in \mathcal{Q}^*$.

2.5. Complementary flow

The above discussion emphasizes the importance of retaining $u(t)$ to be in $\mathcal{Q}^*$. Following Remark 1 we define a complementary flow that aims at maintaining $E(u) \to 0$ without changing the value of $J(u)$. Let us first compute the variational derivative of $E(u)$:

$$\partial_u E = \sum_i \langle Q(u), e_i \rangle \cdot \partial Q_i(u), \tag{11}$$

where

$$\partial Q_i = \sum_j (-1)^j \frac{d^j}{dx^j} \left(\frac{\partial Q}{\partial u^{(j)}} e_i \right),$$

and $u^{(j)}$ denotes the jth derivative of u. We would like the complementary flow not to interfere with the main flow, and specifically not to increase J. A flow that decreases $E(u)$ on one hand and retains $J(u)$ unaffected on the other hand is:

$$u_t = C(u) \tag{12}$$

where

$$C(u) = -\partial_u E + \frac{\langle \partial_u E, T(u) \rangle}{\|T(u)\|^2} T(u).$$

Let us compute the time derivatives of J and E:

$$\begin{aligned} \frac{d}{dt} J(u) &= \langle T(u), u_t \rangle = \langle T(u), C(u) \rangle \\ &= \langle T(u), -\partial_u E + \frac{\langle \partial_u E, T(u) \rangle}{\|T(u)\|^2} T(u) \rangle = 0. \end{aligned} \tag{13}$$

We assume the conditions of the "chain rule" of Eq. (5) hold for the energy $E(u)$. Then for E we have,

$$\begin{aligned} \frac{d}{dt} E(u) &= \langle \partial_u E, u_t \rangle = \langle \partial_u E, C(u) \rangle \\ &= - \|\partial_u E\|^2 + \frac{\langle \partial_u E, T(u) \rangle^2}{\|T(u)\|^2} \leq 0, \end{aligned} \tag{14}$$

where the last inequality follows from Cauchy–Schwarz. Thus in the flow of (12) $E(u(t))$ decreases with time whereas the value of $J(u(t))$ is unchanged. Note that one should verify that $\partial_u E$ and $\partial_u J$ are not exactly parallel with opposite directions. The relations between $\partial_u E$ and $\partial_u J$ are farther discussed in Sec. 5.

3. Combined flows

Constrained optimization problems in variational calculus are well studied, see e.g. [34–36]. In light of Proposition 1 we would like our flow (7) to be constrained to $u \in \mathcal{Q}^*$. Otherwise, we will either not reach a steady state or reach a trivial one (an eigenfunction of zero eigenvalue), which is usually not of interest. Such constrained flows are tied, though not equivalent, to exact penalty methods, as in [35,36]. Inspired by these works, we couple the main flow (7) and the complementary flow (12) as follows,

$$u_t = M(u) + \alpha C(u), \tag{15}$$

where $\alpha \in \mathbb{R}_+$ and $M(u)$ and $C(u)$ are as defined in the contexts of Eqs. (7) and (12), respectively. This combined flow should retain the properties of the main flow, while keeping $E(u)$ zero (for α large enough). Let us now show that $(d/dt)E(u)$ and $(d/dt)J(u)$ are nonpositive:

$$\frac{d}{dt} J(u(t)) = \langle T(u), u_t \rangle = \underbrace{\langle T(u), M(u) \rangle}_{\leq 0} + \alpha \underbrace{\langle T(u), C(u) \rangle}_{=0} \leq 0.$$

$$\frac{d}{dt}E(u(t)) = \langle \partial_u E, u_t \rangle = \langle \partial_u E, M(u) \rangle + \alpha \langle \partial_u E, C(u) \rangle$$

$$= \langle \partial_u E, s \frac{Q(u)}{\|Q(u)\|} - \frac{T(u)}{\|T(u)\|} \rangle + \alpha \left(-\|\partial_u E\|^2 + \frac{\langle \partial_u E, T(u) \rangle^2}{\|T(u)\|^2} \right)$$

$$\leq \|\partial_u E\| - \frac{\langle \partial_u E, T(u) \rangle}{\|T(u)\|} + \alpha \left(-\|\partial_u E\|^2 + \frac{\langle \partial_u E, T(u) \rangle^2}{\|T(u)\|^2} \right)$$

$$= \underbrace{\left(-\|\partial_u E\| + \frac{\langle \partial_u E, T(u) \rangle}{\|T(u)\|} \right)}_{\leq 0} \left(-1 + \alpha \left(\|\partial_u E\| + \frac{\langle \partial_u E, T(u) \rangle}{\|T(u)\|} \right) \right).$$

The inequality of the third row is based on Cauchy–Schwarz inequality, $s\langle \partial_u E, Q(u) \rangle / \|Q(u)\| \leq \|\partial_u E\|$. If $\alpha \gg 1$ and the elements $\partial_u E(u)$ and $T(u)$ are not collinear (in opposite directions) we can deduce that:

$$\frac{d}{dt}E(u(t)) \leq 0.$$

Let us make some notes: First, the parameter α is to limit the main flow to be in the domain of $\mathcal{Q}^*$. In the next sections we show how to simplify this flow in the discrete setting as well as the requirement on α. The combined flow has the same pattern as in the exact penalty algorithm [35]. In that work the minimum of $J(u)$ is constrained by requiring $u \in \mathcal{D} \subset \mathcal{U}$. The essence of the exact penalty algorithm is to run the flow until equilibrium at each iteration. This equilibrium serves as the initial condition for the next iteration with increased α. However, this strategy does not fit our problem. For most values of α reaching equilibrium means u is not in $\mathcal{Q}^*$ and therefore we reach a trivial solution $T(u) = Q(u) = \lambda = 0$.

With respect to the sets $\mathcal{T}^\perp$ and $\mathcal{Q}^*$ (Definition 1 and Definition 3), we note that if $ker\{J\}$ has only a single element then the dimension of $\mathcal{T}^\perp$ is zero and therefore the basis of $\mathcal{T}^\perp$ is an empty set. Consequently, $\mathcal{Q}^*$ coincides with $\mathcal{U}$ and the combined flow degenerates to being the main flow solely.

3.1. Towards a discrete setting

We propose in Algorithm 1 the general discrete iterations that approximate the combined flow of (15). It is based on an explicit scheme for the time discretization. An illustration of Algorithm 1 is shown in Fig. 1.

Instead of choosing a specific α, we split the combined flow back to the main and complementary flows that are invoked alternatingly. In the continuous setting, as discussed above, $M(u)$ decreases the value of $J(u)$ but might cause u to be out of $\mathcal{Q}^*$. The complementary flow, $C(u)$, "returns" u to $\mathcal{Q}^*$ leaving $J(u)$ unchanged. Thus, for each infinitesimal step dt_M in the main flow $M(u)$ (Line 7 in Algorithm 1) the complementary flow is repeatedly invoked (dt_C each time) until u is sufficiently close to $\mathcal{Q}^*$ (the inner loop in Algorithm 1). The time step parameters dt_C and dt_M are not resolved here. A full analysis and bounds on these time steps are given next, for the classical case of $T(u) = -\Delta u$.

The outer loop in Algorithm 1 is repeated until the solution is sufficiently close to an eigenpair in terms of the respective angle. Our stopping condition is based on the absolute angle between $T(u)$ and $Q(u)$,

$$|\cos(\theta)| = \frac{|\langle T(u), Q(u) \rangle|}{\|T(u)\| \cdot \|Q(u)\|}. \tag{16}$$

When the angle θ is zero, T and Q are collinear, and an exact eigenpair is attained. For numerical purposes, we seek a good approximation and stop when θ is below a certain threshold. Further discussions related to the stopping condition are in Appendix A.

Algorithm 1 Eigenpair generating flow.

1: **Inputs:**
    u^0
2: **Initialize:**
    δ, θth   stop conditions
    Compute θ^0 according Eq. (16)
3: **while** $\theta^k > \theta$th **do**
4:     **while** $E(u) > \delta$ **do**
5:         $u^{k,l} = u^{k,l-1} + u_t^{k,l-1} \cdot dt_C$ (complementary flow)
6:     **end while**
7:     $u^{k+1} = u^k + u_t^k \cdot dt_M$ (main flow)
8:     Compute θ^{k+1} according Eq. (16)
9: **end while**

(a) J functional contour   (b) The combined flow as finite state machine
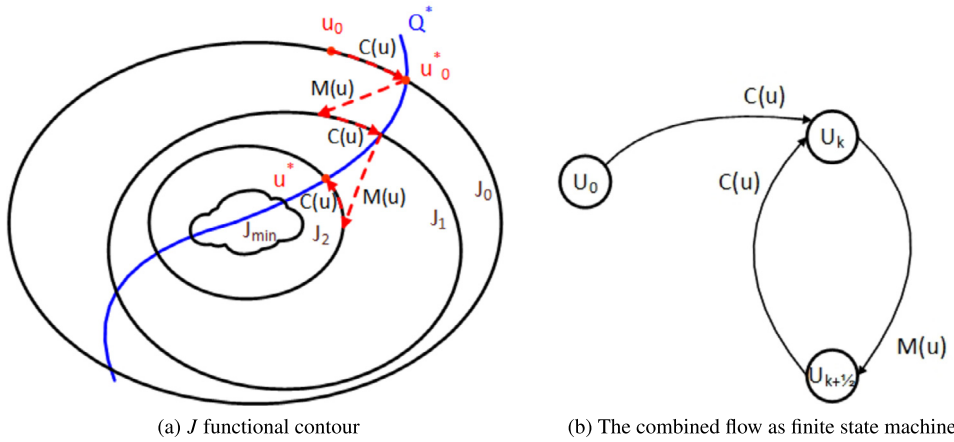
Fig. 1. An illustration of the infinitesimally approximation of the combined flow.

3.2. Realization for $T(u) = -\Delta u$

As many phenomena are based on eigenpairs, in the sense of Eq. (1), with $T(u)$ the negative Laplacian operator, we devote the rest of this paper to that particular case. In this case J is the Dirichlet energy,

$$J(u) = \frac{1}{2}\|\nabla u\|^2.$$

It is clear that J admits the conditions of Eq. (1) and Eq. (5). The null space of the Dirichlet energy is all functions in $\mathcal{U}$ of constant value. According to Corollary 2 it coincides with $\mathcal{T}^{\perp}$. Therefore,

$$\mathcal{T}^{\perp} = \{v \in U : v = const\}.$$

The orthonormal basis of $\mathcal{T}^{\perp}$ is

$$\mathcal{B} = \left\{\frac{1}{\sqrt{|\Omega|}}\right\}.$$

The energy functional $E(u)$ is defined by,

$$E(u) = \frac{1}{2|\Omega|}\langle Q(u), 1\rangle^2,$$

$$\partial E = \frac{1}{|\Omega|}\langle Q(u), 1\rangle \partial Q,$$

and ∂Q is the variational derivative of $\langle Q(u), 1\rangle$. Naturally, $\mathcal{Q}^*$ is the set of all $u \in \mathcal{U}$ such that $\int_{\Omega} Q(u)\,d\mathbf{x} = 0$. The main and complementary operators, respectively, are,

$$M(u) = s\frac{Q(u)}{\|Q(u)\|} + \frac{\Delta u}{\|\Delta u\|}, \tag{17}$$

where $s = \mathrm{sign}(\langle Q(u), -\Delta u\rangle)$, and

$$C(u) = -\partial_u E + \frac{\langle \partial_u E, \Delta u\rangle}{\|\Delta u\|^2}\Delta u. \tag{18}$$

In the following section we resolve the time step sizes for the discrete implementation when T is the negative Laplacian operator.

4. Implementation for the Laplacian operator

For the discrete implementation of the flow we follow the general algorithm presented in the previous section. However, instead of performing a full iterative process of the complementary flow for each main time step, we perform a single step. It is shown that for $T = -\Delta$, with an appropriate time step of the complementary flow, the energy E vanishes, up to a first order Taylor approximation. We suggest the following iterations to approximate the combined flow: Initialize with u^0, iterate until convergence,

$$u^{k+\frac{1}{2}} = u^k + M(u^k) \cdot dt_M$$
$$u^{k+1} = u^{k+\frac{1}{2}} + C(u^{k+\frac{1}{2}}) \cdot dt_C,$$

(19)

where

$$M(u^k) = s \frac{Q(u^k)}{\|Q(u^k)\|} + \frac{\Delta u^k}{\|\Delta u^k\|}$$
$$s = \text{sign}(\langle Q(u^k), -\Delta u^k \rangle), \text{ and}$$
$$C(u^{k+\frac{1}{2}}) = -\partial_u E(u^{k+\frac{1}{2}}) + \frac{\langle \partial_u E(u^{k+\frac{1}{2}}), \Delta u^{k+\frac{1}{2}} \rangle}{\|\Delta u^{k+\frac{1}{2}}\|^2} \Delta u^{k+\frac{1}{2}}.$$

In the rest of this section we set bounds for dt_M and dt_C, to ensure stable flows. These bounds guarantee that in every cycle (from k to $k+1$) we obtain $J(u^k) - J(u^{k+1}) \le 0$ and $E(u^k) \cong 0$, $\forall k$.

4.1. Characterization of $J(u)$ and $E(u)$ within the discrete setting

We now proceed with analyzing the behavior of $J(u^k)$ and $E(u^k)$ using the iterations of (19), where $M(u^k)$ and $C(u^k)$ are defined by (17) and (18). For simplicity, we use the same notations of gradient (∇) and Laplacian (Δ) for the discrete operators.

4.1.1. Main flow iteration
We first analyze the influence of an iteration of the main flow (first row of Eq. (19)) on the functional J. We use the standard first order backward difference time-step approximation of explicit schemes. We examine the change in J at iteration k, denoted by D_J^k, following a time step of the main flow:

$$D_J^k := J(u^{k+\frac{1}{2}}) - J(u^k)$$
$$= J\left(u^k + dt_M \cdot M(u^k)\right) - J(u^k).$$

Using the identity $J(u) = \frac{1}{2}\langle -\Delta u, u \rangle$ yields:

$$D_J^k = \frac{1}{2}\left(\langle -\Delta\left(u^k + dt_M \cdot M(u^k)\right), u^k + dt_M \cdot M(u^k)\rangle - \langle -\Delta u^k, u^k\rangle\right)$$
$$= dt_M\langle -\Delta u^k, M(u^k)\rangle + \frac{1}{2}dt_M^2\|\nabla M(u^k)\|^2.$$

(20)

According to Theorem 1 the expression $\langle \Delta u^k, M(u^k)\rangle$ is non-negative, thus, if

$$0 \le dt_M \le 2\frac{\langle \Delta u^k, M(u^k)\rangle}{\|\nabla M(u^k)\|^2}$$

(21)

then $D_J^k \le 0$.

Let us now examine the influence of the main flow on the functional E. We assume $E(u^k)$ is approximately zero (up to a first order Taylor approximation), to be justified in the next paragraph. The Taylor approximation of $E(u^{k+\frac{1}{2}})$ is given by:

$$E(u^{k+\frac{1}{2}}) = \frac{1}{2|\Omega|}\langle Q(u^{k+\frac{1}{2}}), 1\rangle^2$$
$$= \frac{1}{2|\Omega|}\langle Q(u^k + dt_M M(u^k)), 1\rangle^2$$
$$= \frac{1}{2|\Omega|}\left(\langle Q(u^k), 1\rangle + dt_M\langle \partial Q(u^k), M(u^k)\rangle + O(dt_M^2)\right)^2$$
$$\cong \frac{1}{2|\Omega|}\left(\langle Q(u^k), 1\rangle + dt_M\langle \partial Q(u^k), M(u^k)\rangle\right)^2$$

Under the assumption $E(u^k)$ is approximately zero (i.e. $\langle Q(u^k), 1\rangle \cong 0$) we have,

$$D_E^k := E(u^{k+\frac{1}{2}}) - E(u^k)$$
$$\cong E(u^{k+\frac{1}{2}})$$
$$\cong dt_M^2 \cdot \frac{\langle \partial Q(u^k), M(u^k)\rangle^2}{2|\Omega|}.$$

(22)

This expression emphasizes that $E(u^{k+\frac{1}{2}})$ increases as the time step along the main flow grows.

4.1.2. Complementary flow iteration

We now analyze the influence of the complementary flow (second row of Eq. (19)) on the energies J and E. Here we begin with the analysis of $E(u)$.

$$
\begin{aligned}
D_E^{k+\frac{1}{2}} &:= E(u^{k+1}) - E(u^{k+\frac{1}{2}}) \\
&= E(u^{k+\frac{1}{2}}) + dt_C \cdot \langle \partial E(u^{k+\frac{1}{2}}), C(u^{k+\frac{1}{2}}) \rangle + O(dt_C^2) - E(u^{k+\frac{1}{2}}) \\
&\cong dt_C \cdot \langle \partial E(u^{k+\frac{1}{2}}), C(u^{k+\frac{1}{2}}) \rangle.
\end{aligned}
$$

The step size for which $E(u^{k+1})$ vanishes, as a first order approximation, is therefore

$$
dt_C = -\frac{E(u^{k+\frac{1}{2}})}{\langle \partial E(u^{k+\frac{1}{2}}), C(u^{k+\frac{1}{2}}) \rangle}. \tag{23}
$$

The step size dt_C is positive since the denominator is negative (according to Eq. (19)). Substituting Eq. (22) in Eq. (23) yields the relation between the step sizes of the two flows:

$$
dt_C \cong -dt_M^2 \cdot \frac{\langle \partial Q(u^k), M(u^k) \rangle^2}{2|\Omega| \cdot \langle \partial E(u^{k+\frac{1}{2}}), C(u^{k+\frac{1}{2}}) \rangle}.
$$

Finally, we examine the influence of the complementary flow on the functional J. The change of J along one time step of the complementary flow is

$$
\begin{aligned}
D_J^{k+\frac{1}{2}} &:= J(u^{k+1}) - J(u^{k+\frac{1}{2}}) \\
&= \frac{1}{2}\left(\langle -\Delta u^{k+1}, u^{k+1} \rangle - \langle -\Delta u^{k+\frac{1}{2}}, u^{k+\frac{1}{2}} \rangle \right) \\
&= \frac{1}{2}\left(\langle -\Delta(u^{k+\frac{1}{2}} + dt_C \cdot C(u^{k+\frac{1}{2}})), u^{k+\frac{1}{2}} + dt_C \cdot C(u^{k+\frac{1}{2}}) \rangle - \langle -\Delta u^{k+\frac{1}{2}}, u^{k+\frac{1}{2}} \rangle \right).
\end{aligned}
$$

Note that according to Eq. (19) $\langle \Delta u^{k+\frac{1}{2}}, C(u^{k+\frac{1}{2}}) \rangle = 0$ and therefore

$$
D_J^{k+\frac{1}{2}} = dt_C^2 \|\nabla C(u^{k+\frac{1}{2}})\|^2.
$$

Using Eq. (23),

$$
D_J^{k+\frac{1}{2}} = E^2(u^{k+\frac{1}{2}}) \frac{\|\nabla C(u^{k+\frac{1}{2}})\|^2}{\langle \partial E(u^{k+\frac{1}{2}}), C(u^{k+\frac{1}{2}}) \rangle^2}. \tag{24}
$$

4.1.3. Conditions for the monotonic decrease of J

Following the above constraints on the time step sizes of both flows we can now analyze the change in J for the entire flow, Eq. (19),

$$
J(u^{k+1}) - J(u^k) = D_J^{k+\frac{1}{2}} + D_J^k. \tag{25}
$$

We would like to find a bound on dt_M which ensures $J(u^{k+1}) - J(u^k) \leq 0$. Substituting for $D_J^{k+\frac{1}{2}}$ and D_J^k by Eqs. (24) and (20), respectively, we have,

$$
J(u^{k+1}) - J(u^k) = E^2(u^{k+\frac{1}{2}}) \frac{\|\nabla C(u^{k+\frac{1}{2}})\|^2}{\langle \partial E(u^{k+\frac{1}{2}}), C(u^{k+\frac{1}{2}}) \rangle^2} + dt_M \langle -\Delta u^k, M(u^k) \rangle + \frac{1}{2} dt_M^2 \|\nabla M(u^k)\|^2.
$$

The term $E(u^{k+\frac{1}{2}})$ is evaluated according to the first order approximation of Eq. (22) to obtain,

$$
\begin{aligned}
J(u^{k+1}) - J(u^k) \cong\ & dt_M^4 \cdot \frac{\langle \partial Q(u^k), M(u^k) \rangle^4}{4|\Omega|^2} \cdot \frac{\|\nabla C(u^{k+\frac{1}{2}})\|^2}{\langle \partial E(u^{k+\frac{1}{2}}), C(u^{k+\frac{1}{2}}) \rangle^2} + \\
& dt_M \langle -\Delta u^k, M(u^k) \rangle + \frac{1}{2} dt_M^2 \|\nabla M(u^k)\|^2.
\end{aligned} \tag{26}
$$

A deeper analysis shows that when the directions of $\partial E(u)$ and Δu are far enough from being collinear the fourth order term is small and thus can be omitted. After neglecting the fourth order term on the right-hand-side of eq. (26) the inequality coincides with Eq. (21). We now use the following inequality based on the operator norm of the discrete gradient:

$$\|\nabla u\|^2 \le \frac{4d}{h^2}\|u\|^2, \tag{27}$$

where d is the dimension and h is the spatial grid size. Based on the expression on the right-hand-side of Eq. (21), and the definition of $M(u)$ for the Laplacian case, (17), we have

$$2\frac{\langle \Delta u^k, M(u^k)\rangle}{\|\nabla M(u^k)\|^2} \ge \frac{h^2}{2d}\frac{\langle \Delta u^k, M(u^k)\rangle}{\|M(u^k)\|^2} = \frac{h^2}{2d}\frac{\frac{|\langle \Delta u^k, Q(u^k)\rangle|}{\|Q(u^k)\|} + \|\Delta u^k\|}{2 + 2\frac{|\langle \Delta u^k, Q(u^k)\rangle|}{\|\Delta u^k\|\cdot\|Q(u^k)\|}} = \frac{h^2}{4d}\|\Delta u^k\|. \tag{28}$$

Therefore, to ensure the expression in (26) is negative, we set the following bound on the time step size,

$$dt_M \le \frac{h^2}{4d}\|\Delta u^k\|. \tag{29}$$

According to Eq. (20), D_J^k depends on dt_M quadratically, therefore, the optimal dt_M is half of the upper bound. Consequently, we choose

$$dt_M = \frac{h^2}{8d}\|\Delta u^k\|. \tag{30}$$

Typical values of dt_M in our experiments were in the range $[0.002, 0.6]$ for one dimension and $[0.05, 0.13]$ for two dimensions. These values highly depend on the noise level. A detailed description of the algorithm, in the case of the Laplacian operator, is presented in Algorithm 2.

Algorithm 2 Eigenpair generation for the Laplacian operator.

1: **Inputs:**
    u^0
2: **Initialize:**
    $C(u^0)$,   Eq. (18)
    dt_C,   Eq. (23)
    $u^1 = u^0 + C(u^0)\cdot dt_C$
    Set threshold θ^{th}
    θ^1,   Eq. (16)
3: **while** $\theta^{th} < \theta^k$ **do**
4:     $u^{k+\frac{1}{2}} = u^k + dt_M \cdot M(u^k)$,   Eq. (30)
5:     $C(u^{k+\frac{1}{2}})$,   Eq. (18)
6:     dt_C,   Eq. (23)
7:     $u^{k+1} = u^{k+\frac{1}{2}} + C(u^{k+\frac{1}{2}})\cdot dt_C$
8:     θ^{k+1},   Eq. (16)
9: **end while**

4.2. Interpretations

Let us revisit Eq. (1) and the main flow. Given u^k we can evaluate the eigenvalue according to Eq. (9) and define the error of the solution u^k as:

$$err(u^k) = -\Delta u^k - \lambda(u^k)\cdot Q(u^k) \tag{31}$$

which is zero if u^k is an eigenfunction. In addition, by using the expression of dt_M in Eq. (30), we can calculate the change of u at the kth step as,

$$\begin{aligned} u^{k+\frac{1}{2}} - u^k &= M(u^k)\cdot dt_M \\ &= \frac{h^2}{8d}\left(\Delta u^k + sign(\langle Q(u^k), -\Delta u^k\rangle)\frac{\|\Delta u^k\|}{\|Q(u^k)\|}Q(u^k)\right) \\ &= \frac{h^2}{8d}\left(\Delta u^k + \lambda(u^k)\cdot Q(u^k)\right) \\ &= -\frac{h^2}{8d}\cdot err(u^k). \end{aligned} \tag{32}$$

We note that [7] suggests a general eigenvalue approximation by: $\lambda(u) = \langle -\Delta u, f(u)\rangle / \langle Q(u), f(u)\rangle$ with an arbitrary operator $f(u)$ as long as this ratio exists. In particular we can have $f(u) = u$. Then we can replace Line 4 in Algorithm 2 with Eq. (32) using other eigenvalue evaluations. We can conclude that any flow in the sense of Eq. (32) with an eigenvalue approximation for which Theorem 1 holds, the later properties of Sec. 2 (Lemma 1 and Proposition 1) also hold. This conclusion is valid not only for $T(u) = -\Delta u$ but for any operator $T(u)$ admitting Eq. (1). However, different step size constraints should be found.

5. Applications

In this section we present several numerical experiments using the proposed method. We compare our results with NCGM introduced in [12]. NCGM assumes the eigenvalue is given, therefore we supply the correct eigenvalue to the algorithm. In addition, we compare our method to an adaptive version of NCGM when the eigenvalue is not given (thus the task is to find a full eigenpair, as our flow does). The eigenvalue is approximated at each iteration based on [7]. We denote this method by ANCGM.

5.1. 1 Dimension

5.1.1. Soliton equations

In 1895 *Korteweg and de Vries* (KdV) formulated a mathematical model of waves on shallow water surfaces which were previously described by Russell. Later studies have shown that the KdV equation is the continuum limit of a discrete non-linear mass-spring model [37]. The formulation by Kruskal and Zabusky [38] for such phenomena was:

$$u_t + uu_x + \delta^2 u_{xxx} = 0,$$

with δ a small real scalar. Reformulating this expression for a stationary wave yields the following equation:

$$-u_{XX} = \lambda \left(-cu + \frac{u^2}{2} \right), \tag{33}$$

where c is the wave velocity, $X = x - ct$ and $\lambda = \delta^{-2}$. Naturally, λ can be understood as an eigenvalue. In this example we have $Q(u) = -cu + u^2/2$. The solution to this equation models well a family of solitary waves referred to as solitons, (named by Kruskal and Zabusky). In this case an analytic solution can be formulated, which makes it feasible to compare the experimental results to the ground truth. The solution for (33) is:

$$u(X) = 3c \cdot \mathrm{sech}^2 \left(\frac{\sqrt{c \cdot \lambda} X}{2} \right).$$

The implementation of our flow is based on Algorithm 2, where for solving Eq. (33) we have:

$$Q(u) = -cu + \frac{u^2}{2},$$

$$\partial Q(u) = -c + u,$$

$$\partial_u E = \langle Q(u), 1 \rangle (-c + u).$$

The operators in NCGM [12] are:

$$L = \Delta + \lambda (c - u),$$

$$M = \Delta + \lambda \cdot c,$$

where λ is given. The notations L and M are taken from [12] (not to confuse with $M(u)$ of our algorithm). In the adaptive version, ANCGM, λ is approximated by $\lambda(u) = \langle -\Delta u, u \rangle / \langle Q(u), u \rangle$.

5.1.2. Experimental setup

In our experiments we initialize with a noisy version of the solution, by adding white Gaussian noise N of a certain variance to the analytic solution for some given λ. Note that we also allow some bias in the simulated measurements so the noise mean in not zero. The noise parameters are denoted by a normal distribution $N \sim \mathcal{N}(\mu, \sigma^2)$, with mean μ and variance σ^2. We employ the aforementioned algorithms with a stopping condition $\theta \mathrm{th} \leq 2°$ (where θ is the angle between T and Q, as defined in (16)).

In Fig. 2 the results of the generated eigenfunctions are shown. The noise parameters are $\mu = 0.1$ with variance values of $\sigma^2 = 0.2$ and $\sigma^2 = 0.36$, for the first and second experiments, respectively. For this relatively simple case we compare our results to ANCGM, where both algorithms try to find an eigenpair (λ is not known). We show that our algorithm is quite stable, for different levels of noise. ANCGM on the other hand, collapses to the trivial solution ($-\Delta u = \lambda Q(u) = 0$) for high noise levels (and is less accurate also for moderate noise). We should emphasize that our algorithm runs considerably more iterations than ANCGM. However, our iterations are very fast, as they are based on explicit forward-flow computations, compared to computationally-intensive iterations of ANCGM which involve inversion. Overall, the computations are comparable. The running time (using Matlab code) in the experiment with variance 0.2 are $t = 0.336$ [sec] for ANCGM and $t = 0.1$ [sec] for our algorithm. For variance 0.36, it was $t = 1.7$ [sec] for ANCGM and $t = 1.19$ [sec] for ours.

According to Theorem 1, the main flow reaches a steady state when an eigenpair is attained. Thus, it is expected that if $u_t = 0$ then $sign(\langle Q(u), -\Delta u \rangle) Q(u)/\|Q(u)\| = -\Delta u/\|\Delta u\|$. In Fig. 3 we plotted $sign(\langle Q(u), -\Delta u \rangle) Q(u)/\|Q(u)\|$ and

(a) $N \sim \mathcal{N}(0.1, 0.2)$　　　　　　　　　　(b) $N \sim \mathcal{N}(0.1, 0.36)$
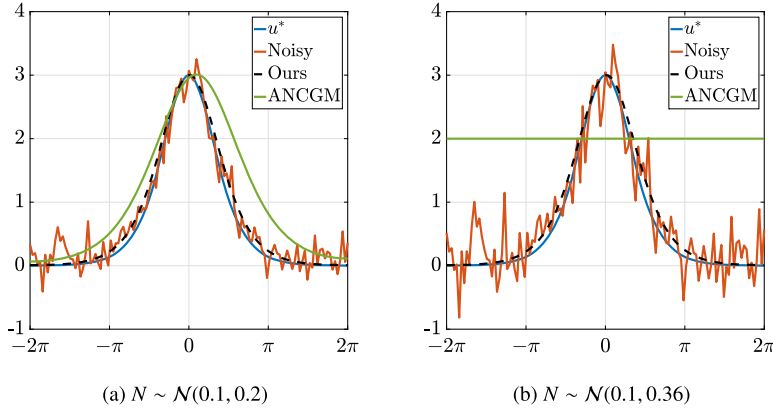
Fig. 2. A comparison of eigenpair generating algorithms for KdV equation with different noise levels. In Fig. 2a we summarize the results of ANCGM and our flow when the initial function u^0, red solid line, is an eigenfunction with additive white Gaussian noise (of mean of 0.1 and variance of 0.2). In Fig. 2b we repeat the experiment with higher level of noise (variance is 0.36). (For interpretation of the colors in the figure(s), the reader is referred to the web version of this article.)


(a) $N \sim \mathcal{N}(0.1, 0.2)$　　　　　　　　　　(b) $N \sim \mathcal{N}(0.1, 0.36)$
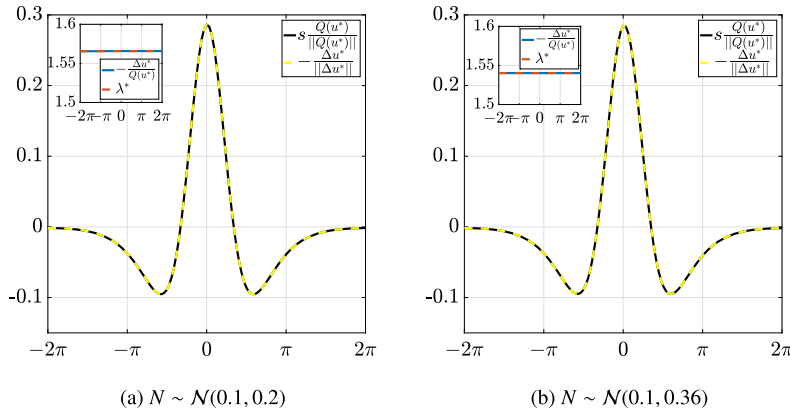
Fig. 3. We show here that our algorithm indeed reaches an eigenpair. The results of $T/\|T\|$ and $sQ/\|Q\|$ are shown when the algorithm converges for the KdV equation. One can observe they coincide very well. The black solid line stands for $sQ(u)/\|Q(u)\|$ and dashed yellow line is $-\Delta u/\|\Delta u\|$. In left top side the approximated $\lambda^* = \langle -\Delta u^*, u^* \rangle / \langle Q(u^*), u^* \rangle$ is plotted with dashed red line and the solid blue line is the ratio $-\Delta u/Q(u)$.

$-\Delta u/\|\Delta u\|$. Moreover, on the top left side of these plots we present the approximated eigenvalue $\lambda = \langle -\Delta u, u \rangle / \langle Q(u), u \rangle$ and the computed pointwise ratio $\lambda(x) = -\Delta u(x)/Q(u(x))$ ($u(x)$ is the result of our algorithm at convergence). One can observe these graphs coincide very well. In Fig. 4 the values of $J(u(t))$ and the mean of $u(t)$ as a function of t are shown. Our theoretical analysis predicts $J(u(t))$ should be decreasing with time (Theorem 1 in the time continuous case and the bound on dt_M of Eq. (29) in the discrete setting). Moreover, since $u(t)$ is very close to $\mathcal{Q}^*$, the mean of $u(t)$ should be almost constant in time (Proposition 1, item 2). It is shown that the numerical implementation approximates well the theoretical analysis.

As opposed to the KdV equation, the analytic solution is usually not known. Here we examine our algorithm using more general initializations. In Figs. 5a to 5c the results of our algorithm are presented when it is initialized with the functions $u(x) = 1 + \cos x/2$, $u(x) = 1 + \cos x$ and $u(x) = 4 \cdot \exp\{-|x|^2\}$, respectively. The results have the same amplitude since we assume the same velocity in the three cases. However, one can observe that different initializations result in a eigenfunctions of different eigenvalues.

5.1.3. Low SNR

An essential assumption of algorithms based on linearization, such as NCGM, is that the initial guess u^0 is close enough to the true solution. In this example we try to demonstrate what happens when this assumption is not valid. In this experiment we initialize with the eigenfunction corresponding to $\lambda = 2$ and $c = 0.25$ and add noise with normal distribution $N \sim \mathcal{N}(0.25, 0.25)$. We compared our algorithm and NCGM, giving both of them this initial function (and additionally providing NCGM the correct λ). Fig. 6 shows the results of this experiment. In Fig. 6a the eigenfunction u^*, the initial function u^0, our algorithm and NCGM results are plotted. Our algorithm converges to another eigenfunction whereas NCGM collapses to a trivial solution. Fig. 6b illustrates the similarity of the two opposite normalized counterparts of the flow u_t,

(a) $N \sim \mathcal{N}(0.1, 0.2)$ (b) $N \sim \mathcal{N}(0.1, 0.36)$
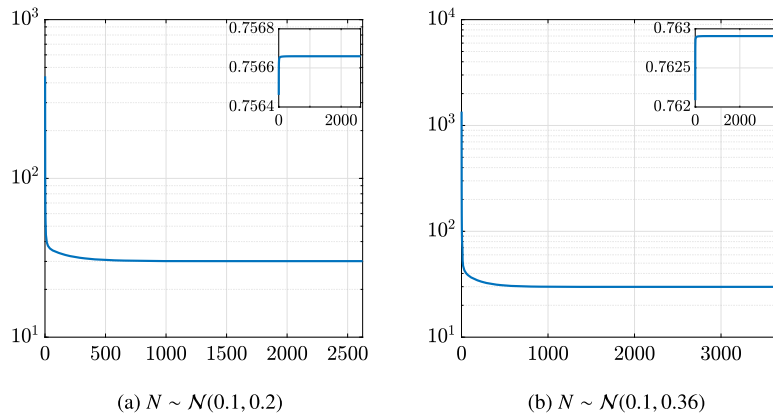
Fig. 4. The value of $J(u^k)$ and the mean of u^k (right top axis) as a function of iteration number k when applying our flow on KdV for the experiments depicted in Fig. 2.

(a)   (b)   (c)
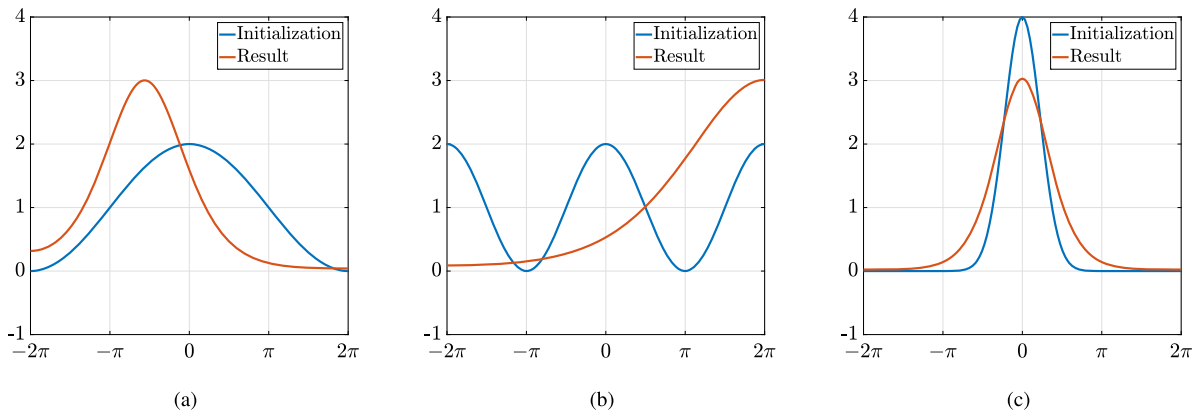
Fig. 5. Different initializations results in different eigenfunctions. In Fig. 5a the initialization is $u = 1 + \cos(x/2)$, in Fig. 5b the initialization is $u = 1 + \cos(x)$ and in Fig. 5c it is $u = 4 \cdot \exp\{-x^2\}$. In all cases we assume the velocity is known (and equal) which results in the same amplitude but having different widths (different eigenvalues).

i.e. $sQ(u)/\|Q(u)\|$ and $-\Delta u/\|\Delta u\|$ showing we indeed approximate an eigenfunction well. In Fig. 6c the value of J and the mean of u are plotted as a function of iteration.

5.1.4. One dimensional nonlinear Schrödinger (NLS) equation

In this part we would like to emphasize the simplicity of our approach. Our algorithm is easy to adjust to other applications and the adjustment amounts to redefining $Q(u)$ and its variational derivative. We demonstrate this by the NLS equation as discussed in [39,40]:

$$i\frac{\partial u}{\partial t} + \frac{\partial^2 u}{\partial x^2} - k|u^2|u = 0.$$

To find a stationary solution we assign $u(x, t) = u(x)e^{i\mu(u)t}$. This yields $-u_{xx} = -\mu(u)u - ku^3$, which can be rewritten as $-u_{xx} = \lambda(-\hat{\mu}(u)u - \hat{k}u^3)$ with $\hat{\mu}(u) = 1 - 3u^2$ and $\hat{k} = 2$. Finally we reach the problem formulation of (1),
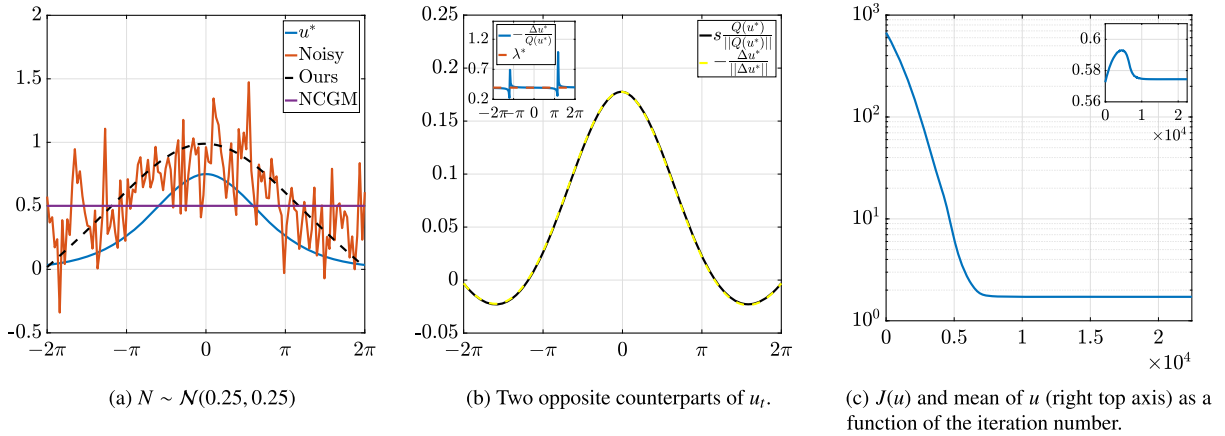
$$-u_{xx} = \lambda(u^3 - u).$$

Therefore, we have

$$Q(u) = u^3 - u,$$

and

$$\partial Q(u) = 3u^2 - 1.$$

(a) $N \sim \mathcal{N}(0.25, 0.25)$

(b) Two opposite counterparts of u_t.

(c) $J(u)$ and mean of u (right top axis) as a function of the iteration number.

Fig. 6. Experiment when the premise $\|u^* - u^0\| << 1$ does not hold. Fig. 6a summarizes the result of NCGM and our flow when the initial function is far from the eigenpair (high level of noise). Whereas NCGM collapses to the trivial solution our flow reaches a meaningful solutions. In Fig. 6b it is demonstrated that a good eigenpair approximation is attained. In Fig. 6c the evolution of J and the mean of u as a function of number of iterations are presented.

(a) Numerical eigenpair result.

(b) Two counterparts of u_t.

(c) J and the mean of u as a function of iteration number.
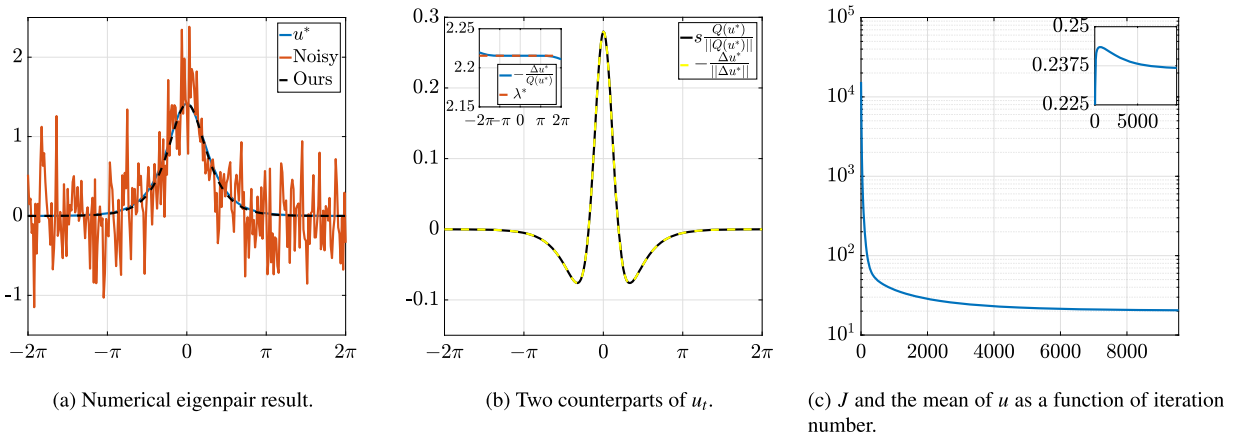
Fig. 7. One dimension NLS equation. The initial function u^0 is an eigenfunction with additive noise, $\mu = 0$, $\sigma^2 = 0.45$. Our algorithm result is shown in Fig. 7a. In Fig. 7b the two counterparts of the main flow are shown when an eigenpair is attained. The functional J and the mean of u are presented in Fig. 7c. NCGM diverges in this experiment and ANCGM converges to a trivial solution ($\lambda = 0$). Both of these results are not in the same scale as the initial signal u^0 and therefore are not presented.

We initiate the algorithm with $u^0 = u^* + N$ where u^* is the eigenfunction $u(x) = \sqrt{2} \operatorname{sech}(\sqrt{\lambda}x)$ and $N \sim \mathcal{N}(0, 0.45)$, see Fig. 7. We similarly initiate the algorithms NCGM and ANCGM. The first diverges and the second one converges to the trivial solution, $\lambda = 0$. Both of these results are not in the same scale as the initial signal and therefore are not plotted.

5.2. Two dimensions NLS equation

The following experiment is based on Example 3.4 from [12] and demonstrates the performance of our algorithm in 2D. We apply our algorithm on NLS equation with periodic potentials which models nonlinear light propagation as well as Bose–Einstein condensate's dynamics in optical lattices. It is formulated as:

$$iU_t + U_{xx} + U_{yy} - V_0\left(\sin^2 x + \sin^2 y\right)U + \sigma|U|^2 U = 0.$$

This equation is discussed in details in [41–43] and admits a rich variety of solitary waves of the form of $U(x, y, t) = u(x, y)e^{-i\mu t}$, where $u(x, y)$ satisfies the equation:

$$u_{xx} + u_{yy} - V_0\left(\sin^2 x + \sin^2 y\right)u + \sigma|u|^2 u = -\mu u.$$

In our example $\mu = 4.11$, $V0 = 6$, $\sigma = 1$ and Dirichlet boundary conditions are used. There is no known analytic solution for these equations. The initial function of our algorithm is $u_0(x, y) = 1.15 \operatorname{sech}(\sqrt{x^2 + y^2})$. The settings for our flow are:
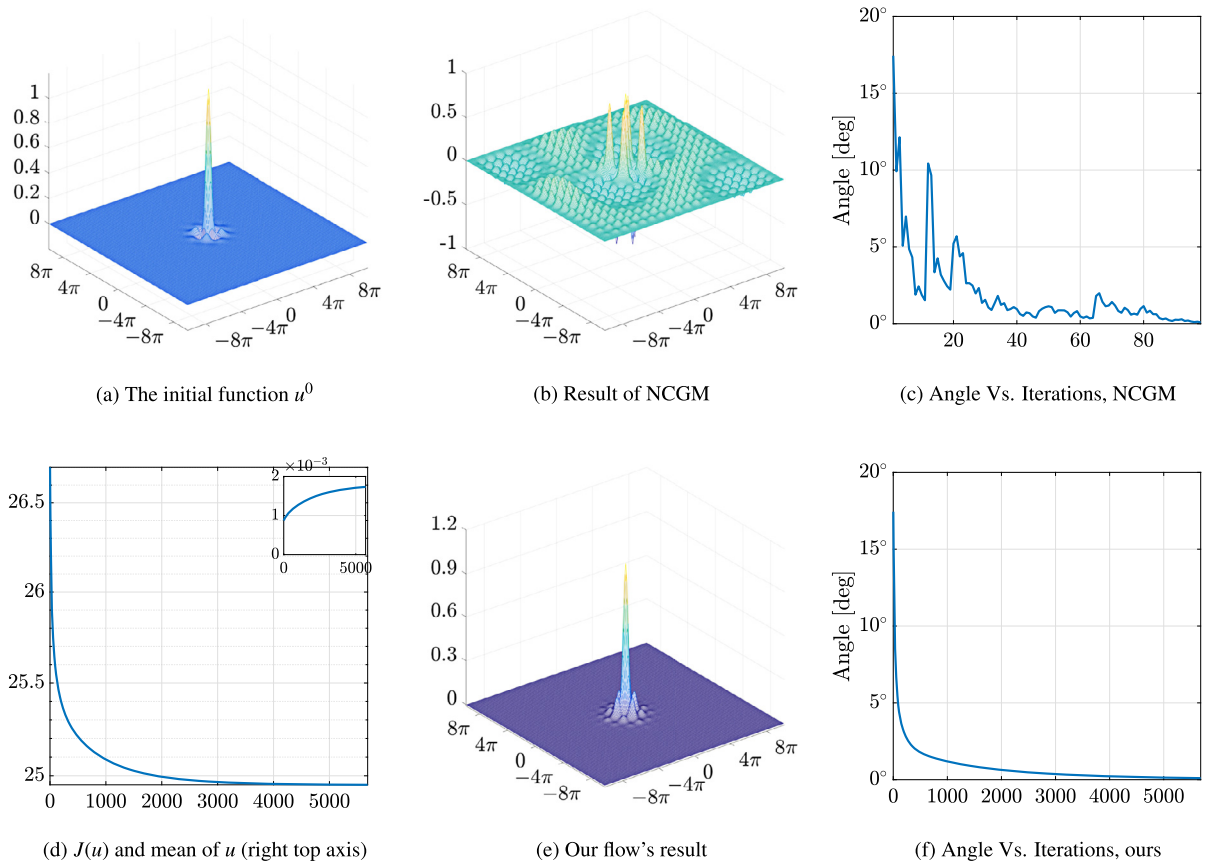
(a) The initial function u^0

(b) Result of NCGM

(c) Angle Vs. Iterations, NCGM

(d) $J(u)$ and mean of u (right top axis)

(e) Our flow's result

(f) Angle Vs. Iterations, ours

Fig. 8. Two dimension NLS.

$$Q(u) = -V_0 \left(\sin^2 x + \sin^2 y \right) u + \sigma u^3 + \mu u,$$

$$\partial Q(u) = -V_0 \left(\sin^2 x + \sin^2 y \right) + 3\sigma u^2 + \mu.$$

The results of our algorithm and NCGM with u^0 are summarized in Fig. 8. In Fig. 8a the initial guess u^0 is shown. The results of NCGM and our flow are presented in Figs. 8b and 8e, respectively, and the angle evolutions along iterations are presented in Figs. 8c and 8f In Fig. 8d we show the behavior of the functional J and the mean of u as a function of time.

We performed a similar experiment of the problem with noise level of $\mathcal{N}(0, 0.0125)$. The result of the experiment are similarly organized in Fig. 9. It is easy to see that NCGM converges approximately to the linear case with very small amplitude signal.

5.3. Decomposition into eigenfunctions

A signal may be modeled in some cases by a linear combination of nonlinear eigenfunctions. In this case we would like to decompose it into its basic elements. We suggest below a simple iterative algorithm to perform that (Algorithm 3). In Fig. 10 we show an example of such a decomposition for the case of KdV. We compute the eigenfunctions ϕ_1, ϕ_2, ϕ_3 with respective eigenvalues $\lambda_1, \lambda_2, \lambda_3$. We used as initial condition a combination of two eigenfunctions of KdV (with eigenvalues $\lambda = 0.25$, $\lambda = 4$). One of them is translated in space (therefore their correlation is low). In the decomposition results, the first two eigenfunctions are very similar to the original ones. The third one is of small amplitude. In that case the linear part becomes dominant and the problem reduces to finding eigenfunctions of the ordinary heat equation. Thus, we get a harmonic function.

Now, we would like to repeat the last experiment for arbitrary signals. We applied Algorithm 3 on uniformly distributed noise in the range $[0, 2]$. In Fig. 11 we show the first four eigenfunctions obtained. It appears that Algorithm 3 is robust enough to handle arbitrary functions. However, we do not have at this stage any guarantee for reconstructing the entire signal, even as $k \to \infty$.
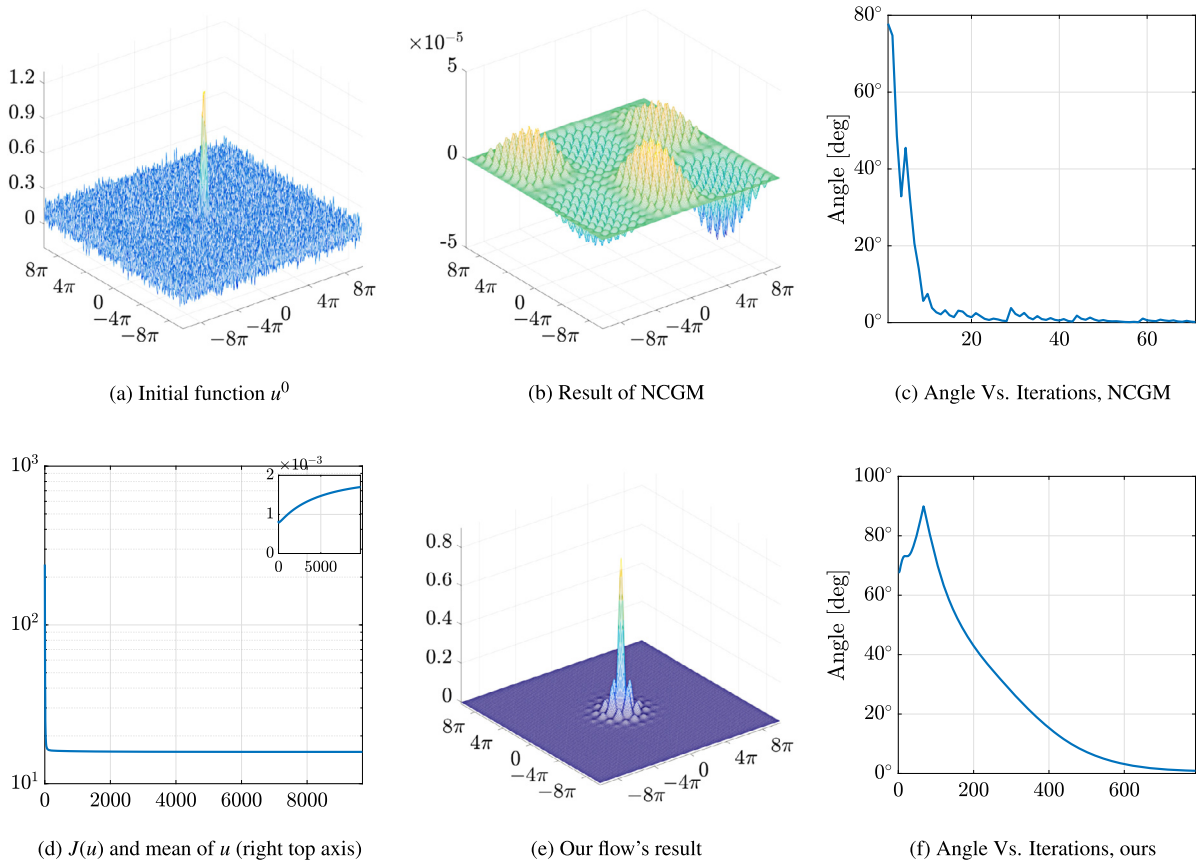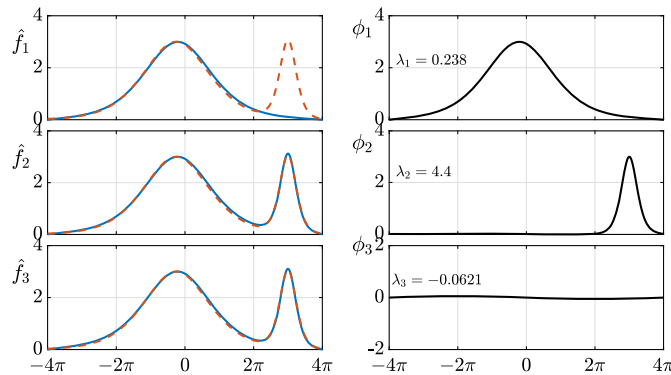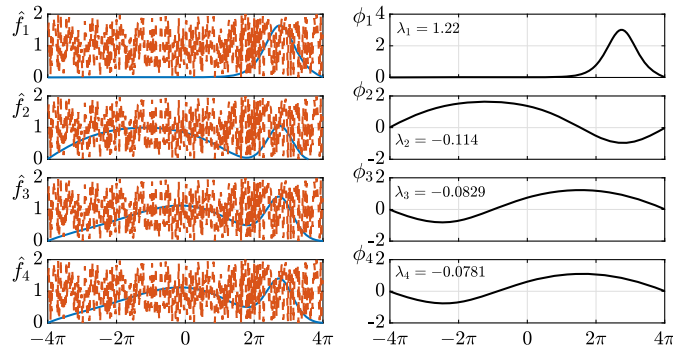
(a) Initial function u^0

(b) Result of NCGM

(c) Angle Vs. Iterations, NCGM

(d) $J(u)$ and mean of u (right top axis)

(e) Our flow's result

(f) Angle Vs. Iterations, ours

Fig. 9. Two dimension NLS with noisy initial function.

Algorithm 3 Nonlinear eigenfunction decomposition.

1: **Inputs:**
  u_0
2: **while** $\|u_{k-1}\| > th$ **do**
3:   Find an eigenpair (ϕ_k, λ_k) using Algorithm 2
4:   $\alpha_k = \frac{\langle u_{k-1}, \phi_k \rangle}{\|\phi_k\|^2}$
5:   $u_k = u_{k-1} - \alpha_k \cdot \phi_k$
6: **end while**
7: Compute the approximated function $\hat{f}_k = \sum_{i=1}^{k} \alpha_k \cdot \phi_k$

Fig. 10. Function decomposition. On the left column, the dashed red line is the initial signal u_0, which is a combination of two eigenfunctions ($\lambda = 0.25$, $\lambda = 4$). The blue solid lines are the reconstructions of the signal up to the kth eigenfunction, i.e. $\hat{f}_k = \sum_{i=1}^{k} \alpha_k \cdot \phi_k$ as described in Algorithm 3. On the right column, we show the eigenfunctions found by Algorithm 3, in the respective order. The first two functions are very similar to the original ones. The third one is a residual function of low amplitude (dominated by the linear part).

Fig. 11. Function decomposition. On the left column, the dashed red line is the initial signal u_0, a uniform noise distributed in the range $[0, 2]$. The blue solid lines are the reconstructions of the signal up to the kth eigenfunction. On the right column, we show the eigenfunctions found by Algorithm 3, in the respective order.

6. Conclusions

In this paper we presented a new nonlinear flow which can generate a very broad family of nonlinear eigenfunctions. The flow reaches a steady state only for eigenpairs. Moreover, the process is a forward flow, which is based on the original operators and does not need their inversion. We thus obtain a very stable process and our assumptions regarding the operators are less restrictive. When T is the negative Laplacian operator, we prove that the flow decreases the Dirichlet energy. This yields a highly stable smoothing process, which is robust to noise.

We introduced the space $\mathcal{Q}^*$, where all nontrivial eigenfunctions reside in, and explained the requirement of the flow to be constrained to this space. A complementary flow was proposed in order to achieve this requirement. We have tested our algorithm on several nonlinear eigenvalue problems in one and two dimensions, and have shown the stability of the algorithm and its robustness to various initial conditions. Finally, it was demonstrated how potentially our process can be used iteratively, in order to decompose a signal into a linear combination of eigenpairs.

Appendix A. Considerations for the stopping condition

Implementations of numerical solutions are concerned with issues related to the appropriate stopping condition. As $T(u)$ and $Q(u)$ are fully correlated when eigensolution of Eq. (1) is attained, the most natural criteria is the angle between them (see Eq. (16)). Other criteria worth mentioning are $(d/dt) J(u)$ Eq. (8) and $\|M(u)\|$ which are shown to be zero when an eigenpair is reached. The norm of the main flow can be calculated as:

$$\|M(u)\| = \sqrt{2}\sqrt{1 - \frac{|\langle Q(u), T(u)\rangle|}{\|Q(u)\| \cdot \|T(u)\|}}. \tag{A.1}$$

If $u \notin \mathcal{Q}^*$ then $\exists e \in \mathcal{B}$ s.t. $\langle Q(u), e\rangle \neq 0$. Let us denote the projection of $Q(u)$ on $\mathcal{T}^\perp$ as:

$$Q^\perp(u) = \sum_{e_i \in \mathcal{B}} e_i \cdot \langle Q(u), e_i\rangle \neq 0,$$

and the "residue" of $Q(u)$ as:

$$Q^\parallel(u) = Q(u) - Q^\perp(u).$$

As $E(u)$ is positive we get the following inequalities:

$$|\cos(\theta)| = \frac{|\langle T(u), Q(u)\rangle|}{\|T(u)\| \cdot \|Q(u)\|} = \frac{|\langle T(u), Q^\parallel(u)\rangle|}{\|T(u)\| \cdot \|Q(u)\|}$$

$$\leq \frac{\|Q^\parallel(u)\|}{\|Q(u)\|} = \frac{\|Q^\parallel(u)\|}{\sqrt{\|Q^\parallel(u)\|^2 + 2E(u)}}$$

and similarly

$$\|M(u)\| = \sqrt{2}\sqrt{1 - \frac{|\langle Q(u), T(u)\rangle|}{\|Q(u)\| \cdot \|T(u)\|}}$$

$$\geq \sqrt{2}\sqrt{1 - \frac{\|Q^\parallel(u)\|}{\sqrt{\|Q^\parallel(u)\|^2 + 2E(u)}}},$$

$$\frac{d}{dt} J(u) \leq \left(\frac{\|Q^{\|}(u)\|}{\sqrt{\|Q^{\|}(u)\|^2 + 2E(u)}} - 1 \right) \|T(u)\|.$$

As long as $E(u) > 0$ our analysis has shown that a precise eigenfunction cannot be obtained. However, one can set a small threshold on $E(u)$, for example, if $E(u) \leq \delta$ we have:

$$\|M(u)\|_{th} = \sqrt{2} \sqrt{1 - \frac{\|Q^{\|}(u)\|}{\sqrt{\|Q^{\|}(u)\|^2 + 4\delta}}}$$

$$\frac{d}{dt} J(u)_{th} = \left(\frac{\|Q^{\|}(u)\|}{\sqrt{\|Q^{\|}(u)\|^2 + 4\delta}} - 1 \right) \|T(u)\| \qquad \text{(A.2)}$$

$$|\cos(\theta)|_{th} = \frac{\|Q^{\|}(u)\|}{\sqrt{\|Q^{\|}(u)\|^2 + 4\delta}}.$$

We note that the above discussion concerns the true evolution in the time continuous setting. However its implications can naturally affect the numerical algorithms.

References

[1] C. Wang, J. Zhou, A new approach for numerically solving nonlinear eigensolution problems, J. Sci. Comput. 64 (2015) 109–129.
[2] C. Effenberger, Robust Solution Methods for Nonlinear Eigenvalue Problems, Ph.D. thesis, EPF Lausanne, 2013.
[3] S. Güttel, F. Tisseur, The nonlinear eigenvalue problem, Acta Numer. 26 (2017) 1–94.
[4] V.I. Petviashvili, Equation of an extraordinary soliton, Fiz. Plazmy 2 (1976) 469–472.
[5] D.E. Pelinovsky, Y.A. Stepanyants, Convergence of Petviashvili's iteration method for numerical approximation of stationary solutions of nonlinear wave equations, SIAM J. Numer. Anal. 42 (2004) 1110–1127.
[6] V. Petviashvili, O. Pokhotelov, Solitary Waves in Plasmas and in the Atmosphere, Gordon and Breach Pub, Co., Reading, 1992.
[7] T.I. Lakoba, J. Yang, A generalized Petviashvili iteration method for scalar and vector hamiltonian equations with arbitrary form of nonlinearity, J. Comput. Phys. 226 (2007) 1668–1692.
[8] J. Álvarez, A. Durán, Petviashvili type methods for traveling wave computations: I. Analysis of convergence, J. Comput. Appl. Math. 266 (2014) 39–51.
[9] J. Álvarez, A. Durán, Numerical generation of periodic traveling wave solutions of some nonlinear dispersive wave systems, J. Comput. Appl. Math. 316 (2017) 29–39.
[10] J. Yang, T.I. Lakoba, Universally-convergent squared-operator iteration methods for solitary waves in general nonlinear wave equations, Stud. Appl. Math. 118 (2007) 153–197.
[11] T.I. Lakoba, Conjugate gradient method for finding fundamental solitary waves, Physica D 238 (2009) 2308–2330.
[12] J. Yang, Newton-conjugate-gradient methods for solitary wave computations, J. Comput. Phys. 228 (2009) 7007–7024.
[13] L.N. Trefethen, D. Bau III, Numerical Linear Algebra, vol. 50, SIAM, 1997.
[14] W. Bao, Q. Du, Computing the ground state solution of Bose–Einstein condensates by a normalized gradient flow, SIAM J. Sci. Comput. 25 (2004) 1674–1697.
[15] J.J. García-Ripoll, V.M. Pérez-García, Optimizing Schrödinger functionals using Sobolev gradients: applications to quantum mechanics and nonlinear optics, SIAM J. Sci. Comput. 23 (2001) 1316–1334.
[16] W. Bao, W. Tang, Ground-state solution of Bose–Einstein condensate by directly minimizing the energy functional, J. Comput. Phys. 187 (2003) 230–254.
[17] M. Caliari, A. Ostermann, S. Rainer, M. Thalhammer, A minimisation approach for computing the ground state of Gross–Pitaevskii systems, J. Comput. Phys. 228 (2009) 349–360.
[18] M. Burger, S. Osher, A guide to the tv zoo, in: Level Set and PDE Based Reconstruction Methods in Imaging, Springer, 2013, pp. 1–70.
[19] L.I. Rudin, S. Osher, E. Fatemi, Nonlinear total variation based noise removal algorithms, Physica D 60 (1992) 259–268.
[20] A. Chambolle, V. Caselles, D. Cremers, M. Novaga, T. Pock, An introduction to total variation for image analysis, Theor. Found. Numer. Methods Sparse Recovery 9 (2010) 227.
[21] Y. Meyer, Oscillating Patterns in Image Processing and Nonlinear Evolution Equations: The Fifteenth Dean Jacqueline B. Lewis Memorial Lectures, American Mathematical Society, Boston, MA, USA, 2001.
[22] F. Andreu, C. Ballester, V. Caselles, J.M. Mazón, Minimizing total variation flow, Differ. Integral Equ. 14 (2001) 321–360.
[23] G. Gilboa, A spectral approach to total variation, in: International Conference on Scale Space and Variational Methods in Computer Vision, Springer, 2013, pp. 36–47.
[24] G. Gilboa, A total variation spectral framework for scale and texture analysis, SIAM J. Imaging Sci. 7 (2014) 1937–1961.
[25] M. Burger, G. Gilboa, M. Moeller, L. Eckardt, D. Cremers, Spectral decompositions using one-homogeneous functionals, SIAM J. Imaging Sci. 9 (2016) 1374–1408.
[26] R.Z. Nossek, G. Gilboa, Flows generating nonlinear eigenfunctions, J. Sci. Comput. (2016) 1–30.
[27] X. Yao, J. Zhou, Numerical methods for computing nonlinear eigenpairs: part I. Iso-homogeneous cases, SIAM J. Sci. Comput. 29 (2007) 1355–1374.
[28] J. Horák, Numerical investigation of the smallest eigenvalues of the p-Laplace operator on planar domains, Electron. J. Differ. Equ. 2011 (2011) 1.
[29] M. Benning, M. Burger, Ground states and singular vectors of convex variational regularization methods, Methods Appl. Anal. 20 (2013) 295–334.
[30] M. Hein, T. Bühler, An inverse power method for nonlinear eigenproblems with applications in 1-spectral clustering and sparse pca, in: Advances in Neural Information Processing Systems, 2010, pp. 847–855.
[31] H. Brezis, Opérateurs maximaux monotones et semi-groupes de contractions dans les espaces de Hilbert, vol. 5, Elsevier, 1973.
[32] V. Apidopoulos, J.-F. Aujol, C. Dossal, On a Second Order Differential Inclusion Modeling the Fista Algorithm, 2017.
[33] J.-F. Aujol, G. Gilboa, N. Papadakis, Theoretical Analysis of Flows Estimating Eigenfunctions of One-Homogeneous Functionals for Segmentation and Clustering, 2017.
[34] I. Ekeland, R. Temam, Convex Analysis and Variational Problems, vol. 28, SIAM, 1999.
[35] V.F. Dem'yanov, Exact penalty functions and problems of variation calculus, Autom. Remote Control 65 (2004) 280–290.
[36] V. Demyanov, G.S. Tamasyan, Exact penalty functions in isoperimetric problems, Optimization 60 (2011) 153–177.
[37] J.A. Pava, Nonlinear Dispersive Equations: Existence and Stability of Solitary and Periodic Travelling Wave Solutions, vol. 156, American Mathematical Soc, 2009.

[38] N.J. Zabusky, M.D. Kruskal, Interaction of "solitons" in a collisionless plasma and the recurrence of initial states, Phys. Rev. Lett. 15 (1965) 240.
[39] A. Shabat, V. Zakharov, Exact theory of two-dimensional self-focusing and one-dimensional self-modulation of waves in nonlinear media, Sov. Phys. JETP 34 (1972) 62.
[40] V.E. Zakharov, S.V. Manakov, On the complete integrability of a nonlinear Schrödinger equation, Theor. Math. Phys. 19 (1974) 551–559.
[41] F. Dalfovo, S. Giorgini, L.P. Pitaevskii, S. Stringari, Theory of Bose–Einstein condensation in trapped gases, Rev. Mod. Phys. 71 (1999) 463.
[42] O. Morsch, M. Oberthaler, Dynamics of Bose–Einstein condensates in optical lattices, Rev. Mod. Phys. 78 (2006) 179.
[43] M. Skorobogatiy, J. Yang, Fundamentals of Photonic Crystal Guiding, Cambridge University Press, 2009.